

A *Drosophila* model for Angelman syndrome

Yaning Wu*, Francois V. Bolduc^{†‡§}, Kimberly Bell^{†*}, Tim Tully^{†*}, Yanshan Fang[¶], Amita Sehgal[¶], and Janice A. Fischer^{*||}

*Section of Molecular Cell and Developmental Biology, Institute for Cell and Molecular Biology, University of Texas, 1 University Station A4800, Austin, TX 78712; [†]Cold Spring Harbor Laboratories, 1 Bungtown Road, Cold Spring Harbor, NY 11724; [‡]Dart Neuroscience, LLC, 7374 Lusk Blvd, San Diego, CA 92121; and [§]Howard Hughes Medical Institute and Department of Neuroscience, University of Pennsylvania School of Medicine, Philadelphia, PA 19104

Communicated by Ruth Lehmann, New York University Medical Center, New York, NY, June 2, 2008 (received for review August 15, 2007)

Angelman syndrome is a neurological disorder whose symptoms include severe mental retardation, loss of motor coordination, and sleep disturbances. The disease is caused by a loss of function of *UBE3A*, which encodes a HECT-domain ubiquitin ligase. Here, we generate a *Drosophila* model for the disease. The results of several experiments show that the functions of human *UBE3A* and its fly counterpart, *dube3a*, are similar. First, expression of *Dube3a* is enriched in the *Drosophila* nervous system, including mushroom bodies, the seat of learning and memory. Second, we have generated *dube3a* null mutants, and they appear normal externally, but display abnormal locomotive behavior and circadian rhythms, and defective long-term memory. Third, flies that overexpress *Dube3a* in the nervous system also display locomotion defects, dependent on the ubiquitin ligase activity. Finally, missense mutations in *UBE3A* alleles of Angelman syndrome patients alter amino acid residues conserved in the fly protein, and when introduced into *dube3a*, behave as loss-of-function mutations. The simplest model for Angelman syndrome is that in the absence of *UBE3A*, particular substrates fail to be ubiquitinated and proteasomally degraded, accumulate in the brain, and interfere with brain function. We have generated flies useful for genetic screens to identify *Dube3a* substrates. These flies overexpress *Dube3a* in the eye or wing and display morphological abnormalities, dependent on the critical catalytic cysteine. We conclude that *dube3a* mutants are a valid model for Angelman syndrome, with great potential for identifying the elusive *UBE3A* substrates relevant to the disease.

E6-AP | *UBE3A* | ubiquitin ligase | mental retardation

Angelman syndrome (AS) is an inherited neurological disorder that occurs in $\approx 1/15,000$ births and is characterized by mental retardation, minimal speech, difficulties in motor coordination, seizures, sleep disorders, and unusual behaviors such as excessive laughter, excitability, and short attention span (1, 2). AS is caused by a loss of function of a single gene on chromosome 15 called *UBE3A*, which encodes a HECT domain ubiquitin ligase or E3 protein (3, 4). Through covalent interactions with the catalytic cysteine residue, HECT domain ligases accept ubiquitin from E2 proteins and transfer the ubiquitin to specific substrates (5). *UBE3A* was originally called E6-AP because it was initially identified through its interactions with the viral E6 protein; binding to E6 subverts the normal substrate specificity of E6-AP to p53, and p53 degradation leads to cervical cancer (6).

There are four genetic mechanisms known for inheritance of AS (1). *UBE3A* is within a region of chromosome 15 that is paternally imprinted in the hippocampus and in the Purkinje cells of the brain (7–9). Thus, mutation of the maternally inherited gene copy underlies all four mechanisms. Most (68%) cases of AS are because of a deletion in the maternal chromosome 15 that includes *UBE3A*. Mutations in the maternal *UBE3A* gene account for another 13% of AS cases, whereas another 6% are because of imprinting defects and repression of the maternal *UBE3A* gene copy. The smallest number (3%) of AS incidences is caused by paternal uniparental disomy for chromosome 15. Finally, 10% of people with clear AS symptoms do not fall into any of the above classes, and the cause of their syndrome is unknown.

Several mouse models of AS have been generated including two simple knockouts of the mouse *UBE3A* homolog on chromosome 7 (10–13). The knockout mutants recapitulate several aspects of the disease; cerebellar and hippocampal morphology are normal, but the mice display motor dysfunction, seizures, and memory defects. Ubiquitination has a variety of effects on protein function, depending on whether a protein is monoubiquitinated or tagged with a ubiquitin chain depending on how the ubiquitin chain is linked (14). *UBE3A* attaches to its substrates ubiquitin chains that are linked through the K48 residue of the first ubiquitin and the terminal G76 of the incoming ubiquitin (15). So-called K48-linked chains usually target substrates for proteasomal degradation. Thus, the simplest model to explain why loss of *UBE3A* activity leads to AS is that in the absence of the ubiquitin ligase, one or more *UBE3A* substrates accumulate in the brain and interfere with brain function. A few *UBE3A* substrates have been identified biochemically, but none of them has been shown to be relevant to AS (16–19).

The *Drosophila* genome has a *UBE3A* homolog called *dube3a* (20–22), and thus *Drosophila* genetics could provide a powerful means to identify *Dube3a* (and *UBE3A*) substrates relevant to AS. Here, we provide compelling evidence that *Drosophila dube3a* mutants are indeed a useful AS model.

Results and Discussion

***Drosophila UBE3A* Homolog *dube3a* Likely Encodes One Protein Expressed Throughout Development.** The *Drosophila* gene *CG6190*, located at polytene position 68B1 on chromosome 3L (23), has been identified as *dube3a* (20–22). There are 14 HECT domain E3 proteins in *Drosophila* (23), and the putative *Dube3a* protein is clearly the most similar to *UBE3A*. The fly and human proteins are similar throughout with the most similarity residing in their C-terminal HECT domains [supporting information (SI) Fig. S1]. Using RT-PCR and DNA sequence determination, we found the predicted *dube3a* mRNA (23) in embryos, larvae, and adults (data not shown).

Generation and Molecular Characterization of *dube3a* Loss-of-Function Alleles. One mutant *dube3a* allele, with a P transposable element inserted in the 5' UTR (23), was available, but *dube3a* expression was not obviously disrupted by the P insertion (data not shown). By mobilizing the P element, we generated three imprecise excision (deletion) alleles: *dube3a*⁸⁰, *dube3a*^{6J}, and *dube3a*^{15B} (Fig. 1A). In addition, we isolated a precise excision (WT) allele called *dube3a*^{6PE} that is isogenic with *dube3a*^{15B} for the two major autosomes. Homozygotes for each of the deletion alleles, or *trans*-heterozygotes of each allele with *Df(3L)vin5*, a

Author contributions: Y.W., F.V.B., Y.F., and J.A.F. designed research; Y.W., F.V.B., K.B., and Y.F. performed research; T.T. and A.S. contributed new reagents/analytic tools; Y.W., F.V.B., Y.F., A.S., and J.A.F. analyzed data; and F.V.B., Y.F., and J.A.F. wrote the paper.

The authors declare no conflict of interest.

[¶]Present address: Division of Pediatric Neuroscience, University of Alberta, Edmonton, AB, T6G 2J3, Canada.

^{||}To whom correspondence should be addressed. E-mail: jaf@mail.utexas.edu.

This article contains supporting information online at www.pnas.org/cgi/content/full/0805291105/DCSupplemental.

© 2008 by The National Academy of Sciences of the USA

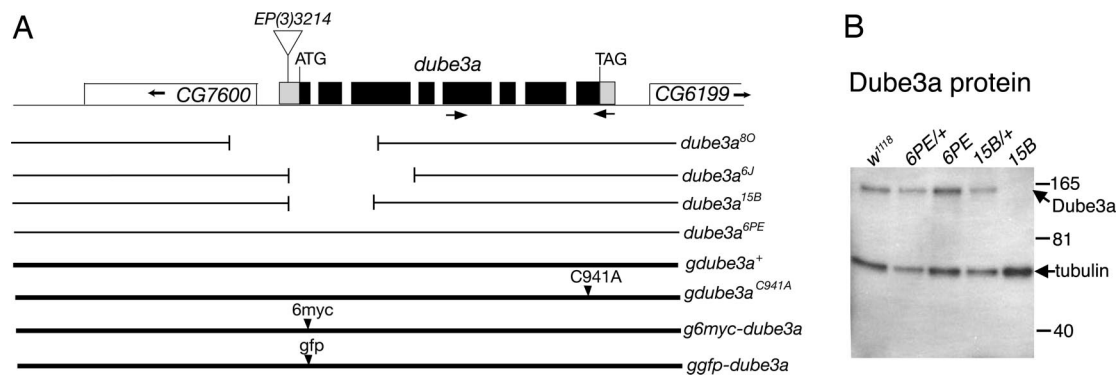


Fig. 1. Characterization of WT and mutant *dube3a* alleles. (A) A diagram of the *dube3a* genomic region is shown at *Upper* (not to scale). There is ≈ 400 bp between CG7600 and *dube3a*, and ≈ 200 bp between CG6199 and *dube3a*. Boxes are exons, black indicates coding region, and gray indicates noncoding regions. The arrows beneath the *dube3a* exons indicate PCR primers used for transcript detection. Extent of the deletions in *dube3a* alleles is indicated: deletion 6J is ≈ 1.7 kb, 80 is ≈ 2.4 kb, and 15B is ≈ 1.2 kb. Black bars beneath indicate the ≈ 12.9 kb genomic DNA fragments in each transgene. (B) Shown is a blot of eye disc protein extracts from third instar larvae. The blots were probed with anti-Dube3a and anti-Tubulin.

chromosome with a deletion that includes *dube3a* and several other genes (23), are viable, fertile, and their external morphology appears normal.

Two alleles, *dube3a*^{6J} and *dube3a*^{15B}, retain the transcription start (Fig. 1A), and transcripts containing exons downstream of the deletions were detected by RT-PCR in these mutant flies (data not shown). In contrast, the transcription start site is within the deletion in *dube3a*⁸⁰, and no *dube3a*⁸⁰ transcripts were detected (data not shown). We used a bacterially produced full-length Dube3a protein to generate polyclonal anti-Dube3a antibodies in rats and guinea pigs. Each antibody recognizes a protein of the expected size (M_r , ≈ 107 kDa) in WT third instar larval eye discs and embryos (data not shown), and neither full-length nor truncated proteins are detected in any of the deletion mutants (Fig. 1B; data not shown). The antibody detects N-terminally truncated Dube3a proteins of M_r ≈ 80 kDa or ≈ 40 kDa produced in bacteria, that begin at either M353, the first methionine residue downstream of the *dube3a*^{15B} deletion breakpoint, or M639 (see Fig. S1; data not shown), respectively. Thus, proteins potentially generated by initiation at downstream start codons in *dube3a*^{6J} or *dube3a*^{15B} mRNAs are unlikely to have escaped detection. We conclude that the antibodies are specific for Dube3a, and that the three deletion mutants likely pro-

duce no protein. All of the behavioral studies were performed with *dube3a*^{15B} (null mutant) and its isogenic counterpart *dube3a*^{6PE} (WT).

Dube3a Expression Is Broad and Mainly Cytoplasmic. AS is associated with loss of UBE3A expression in the developing brain, particularly in the hippocampal and Purkinje neurons, which are the seats of memory and motor coordination, respectively. In mice, UBE3A is broadly expressed early in embryogenesis and later concentrates in neural tissue (11). Thus, we wanted to determine whether Dube3a is expressed in the fly central nervous system during development. Using immunofluorescence, we examined expression in whole-mount embryos, larval brain and ventral nerve cord, larval eye discs, and adult brain. Because the anti-Dube3a signals were robust in embryos only, we generated flies containing genomic DNA transgenes that express N-terminally 6myc- or GFP-tagged Dube3a proteins from the *dube3a* promoter (Fig. 1A).

Embryos were labeled simultaneously with antibodies to Dube3a and the pan-neural nuclear protein, Elav. We find that expression of Dube3a is ubiquitous and cytoplasmic, starting early in embryogenesis and expressed in the developing nervous system (Fig. 2A and B'). The Dube3a antibody is specific in this

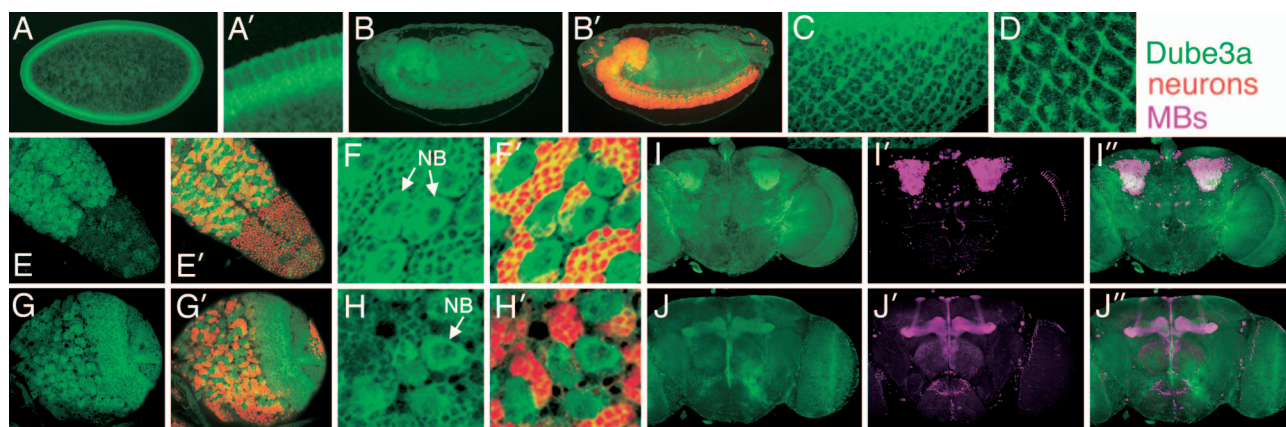


Fig. 2. Dube3a protein in *Drosophila* tissues. Confocal images are shown. (A) A stage 5 embryo. Dube3a accumulates mainly in the cytoplasm and cortically. (A') Enlargement of part of A. (B and B') A stage 15 embryo. Dube3a is expressed broadly, including in Elav⁺ neural cells. (C) GFP-Dube3a expression is ubiquitous and mainly cytoplasmic in third instar larval eye discs. (D) Enlargement of an eye disc expressing 6mDube3a. (E and E') Ventral nerve cord and brain (G and G') of a third instar larva. Dube3a is expressed ubiquitously in the cytoplasm, with elevated levels in the neuroblasts (which are too young to express Elav) and their immediate progeny. (F, F', H, and H') Enlargements of regions in (E and E') and (G and G'), respectively. NB, neuroblasts. (I–J'') show expression in adult brains. Mushroom bodies (MBs) are marked by nuclear GFP expressed by *OK201Y > UAS-nucgfp*. (I and J) show different planes.

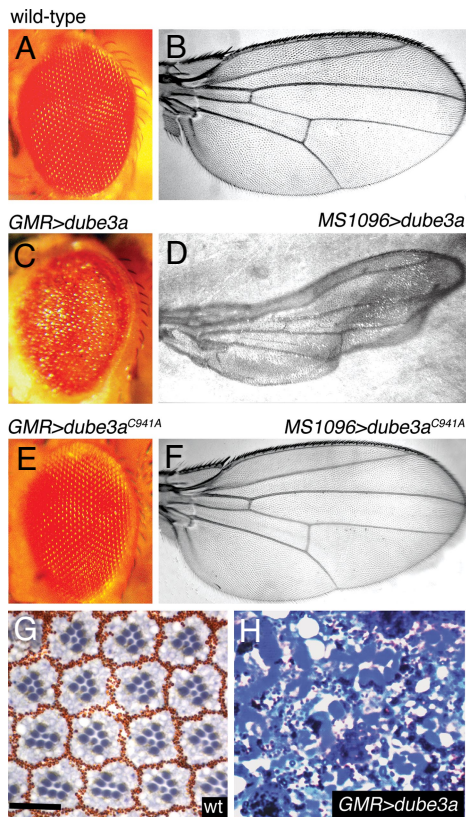


Fig. 4. Morphological defects in flies that overexpress *dube3a*⁺ in the eye or wing. Shown are external eyes (A, C, and E) and wings (B, D, and F) of flies that are WT (A and B) or that overexpress the *UAS* transgene indicated with the eye-specific *Gal4* driver (*GMR-gal4*) or the wing-specific driver (*MS1096-gal4*). In flies with either the *UAS* or the *Gal4* driver alone, eyes and wings are WT. (C and D) Eyes are irregular and wing tissue is curly. (E and F) Eyes and wings are WT. Five different *UAS-dube3a* lines and two different *UAS-dube3a*^{C941A} lines gave the same results as those shown. Ubiquitous overexpression of *Dube3a* by using a *tubulin-gal4* driver and any of the five *UAS-dube3a* lines was lethal, whereas ubiquitous overexpression of *Dube3a*^{C941A} with either of two *UAS-dube3a*^{C941A} lines had no effect. (Scale bar, 200 μ m in A–F) (G and H) Tangential sections through WT eyes or eyes overexpressing *Dube3a*. WT retinas contain organized hexagonal facets, each with eight photoreceptors arranged in a trapezoid. Retinal morphology is severely disrupted by *Dube3a* overexpression (Scale bar, 20 μ m in G and H).

also assayed *Dube3a* protein accumulation in several lines, and representative results are shown in Fig. S7B. We find that two of the mutant proteins, *Dube3a*^{R626C} and *Dube3a*^{I925K}, behave identically to the catalytically inactive *Dube3a*^{C941A} protein in this assay; the mutant proteins accumulate to levels that are similar to WT protein but do not cause a mutant phenotype. *Dube3a*^{C55Y} also behaves like *Dube3a*^{C941A} in that it fails to cause a mutant phenotype, but its level of accumulation is lower than that of *Dube3a*^{C941A} and WT *Dube3a*. Finally, *Dube3a*^{T447P} showed variable results. Four of six lines, at least one of which expresses similar levels of protein to WT *Dube3a* and *Dube3a*^{C941A}, result in no phenotypes. However, one line results in lethality, and one has rough eyes. *Dube3a*^{T447P} may be a partially functional protein that can cause a mutant phenotype only when expressed at higher levels than *Dube3a*. We conclude that the fly counterparts of all four of the disease missense alleles behave as loss-of-function mutations in the fly, probably through a variety of different mechanisms (33) (see *SI Text*).

Flies with *dube3a* Mutations Are Defective in Long-Term Memory Formation. AS patients suffer severe cognitive impairment. *UBE3A* mutant mice may be similarly impaired; they can learn to associate

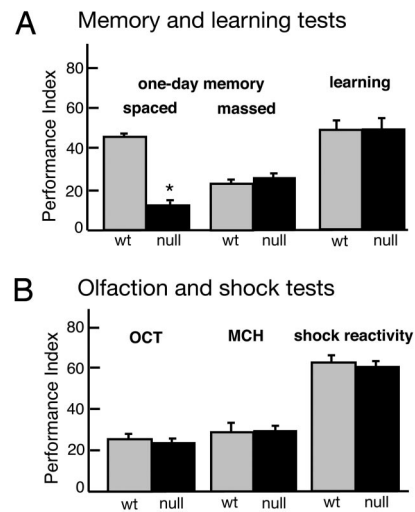


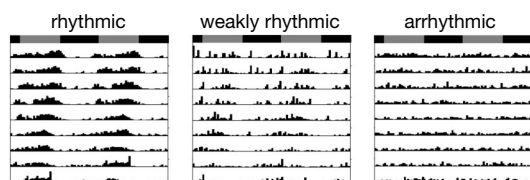
Fig. 5. Defective 1-d memory in *dube3a* mutants specifically after spaced training. (A) Results of 1-d memory and learning tests are shown. *dube3a* null mutants perform worse than WT flies after spaced training but not after massed training or immediately after a single training session (learning) (8 PI per genotype; *, $P < 0.0001$). (B) Results of behavioral experiments for task-relevant olfactory acuity and shock reactivity are shown. No significant differences were observed between *dube3a* null mutants and WT (8 PI per genotype; $P = 0.61$ for 3-octanol (OCT); $P = 0.98$ for 4-methylcyclohexanol (MCH). Aversion to OCT or MCH was similar in mutant vs. control flies ($P = 0.55$ and $P = 0.32$, respectively; data not shown). There is no significant difference between *dube3a* null mutants and WT controls (4 PI per genotype; $P = 0.78$). Error bars, standard error; PI, performance index; OCT, 3-octanol; MCH, 4-methylcyclohexanol. See *Materials and Methods* for complete description of methods and calculation of PI.

a tone with a shock (fear conditioning) but have impaired context dependent long-term memory (LTM) (10). We tested *dube3a* mutant flies for defects in olfactory learning and memory; the flies were trained to associate an odor with a shock and were then tested for avoidance of the odor (34, 35). As in mice, LTM in *Drosophila* requires repeated training (34–36). “Spaced training,” in which 10 training sessions (12 trials in a session) are separated by 15-min rest intervals, produces LTM that requires protein synthesis and lasts more than one week (34–36). In contrast, the same 10 training sessions without the rest intervals, known as “massed training,” induces a different kind of memory that is protein synthesis independent and decays within 4 d (34–36). One-day memory performance is usually higher after spaced training than massed training (34–36). To determine whether *dube3a* mutant flies have memory defects, we tested null mutants for 1-d memory after spaced or massed training, and we found that after spaced training, their memories were significantly defective when compared with WT, but similar to WT after massed training (Fig. 5A). The LTM defect after spaced training cannot be attributed to an inability of *dube3a* flies to react to shock or an olfaction deficit because mutant and WT performed similarly in direct tests of shock reactivity and olfaction (Fig. 5B). Moreover, the memory deficit is not because of failure to learn because immediately after a single training session, null mutants and WT performed similarly (Fig. 5A). The specificity of the defect to spaced training suggests that, similar to *UBE3A* mutant mice, *dube3a* mutant flies learn as well but cannot form LTMs as well as WT flies. Because LTM requires particular transcription factors and protein synthesis (37–39), *Dube3a* activity may be involved in regulation of gene expression.

***dube3a* Null Mutants Have Abnormal Circadian Rhythms.** Because many AS patients suffer sleep disturbance, we asked whether *dube3a* mutant flies are defective in rest/activity rhythms. Flies

Circadian Rhythm Tests

A Activity records



B Rhythm strength

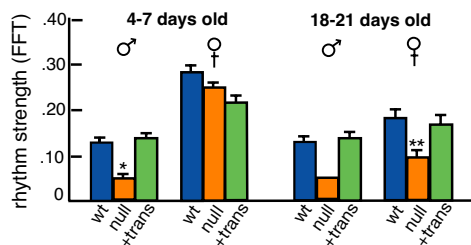


Fig. 6. Rest/activity rhythms are weaker in *dube3a* null flies. (A) Representative locomotor activity records of flies (see *Materials and Methods* for classification criteria). (B) Summary of rhythm strength: wt = *dube3a*^{6PE}, null = *dube3a*^{15B}, and +trans = *dube3a*^{15B} containing one copy of a *gdube3a*⁺ transgene. Relative rhythmicity was evaluated by Fast Fourier Transformation analysis. Error bars are standard error; a bar is absent from 18–21-d males because only one fly was weakly rhythmic. Statistical significance was determined by two-tailed Student's *t* test with unequal variance. *, *P* < 0.01; **, *P* < 0.0001.

were entrained to a 12 h:12 h, light:dark cycle for 3 d before placing them in locomotor activity monitors that record the frequency with which a fly crosses an infrared beam passed through the chamber (40). Activity of the flies was monitored for 12–14 d in constant darkness, which allows for the determination of free-running circadian rhythms. We tested the behavior of *dube3a* null and WT flies, and mutants containing a copy of the *gdube3a*⁺ transgene (Fig. 1A), and used the data to determine the periodicity and strength (consolidation) of the rhythm. Because flies undergo age associated changes in rhythm strength and period, and the pattern of activity varies with gender (41), young (4–7 d) and old (18–21 d) flies of each sex were tested separately. In all three genotypes, we observed periods within the WT range in rhythmic flies (≈ 23.5 h; data not shown). However, when compared with both controls, a larger fraction of *dube3a* mutant males were arrhythmic (Table S1), and rhythm strength was reduced in young males and older flies of both sexes (Fig. 6). Core proteins of the molecular clock are regulated by ubiquitin-mediated proteolysis, and two ubiquitin ligases, Slimb and Jetlag, mediate their degradation (42, 43). More experiments are required to determine whether Dube3a functions similarly.

***dube3a* Mutant Flies Are Not Susceptible to Seizures.** Because many AS patients experience seizures, we also subjected *dube3a* mutant flies to mechanical stress by vortexing them or heat shocking them briefly. Subjecting the flies to mechanical or thermal stress induces paralysis in susceptible flies, a phenomenon that is thought to be related to human seizures (44). *dube3a* mutant flies of two ages were subjected to each stress, and none of the flies showed any signs of paralysis (data not shown). The seizure phenotype is not only variable in AS patients (1, 2) but also in mouse models (10, 13).

Concluding Remarks. We have generated loss-of-function and gain-of-function *dube3a* mutants with great potential for use in genome-wide, genetic screens to reveal substrates of Dube3a and UBE3A relevant to AS. Moreover, the fly model provides a means to test the potential relevance to AS of a Dube3a substrate; overexpression in the brain of relevant substrates should result in behavior defects similar to those observed in *dube3a* loss-of-function mutations. Genes that pass this test can then be tested in the mouse model.

Materials and Methods

Drosophila Genetics. The following strains were obtained from the Bloomington *Drosophila* stock center unless otherwise indicated. *dube3a*^{EP(3)3214} (FBti0011388); *elav-gal4* (FBti0072910); *cha-gal4.7.4* (FBti0024050); *repo-gal4* (FBti0018692); *OK107-gal4* (FBti0004170); *201Y-gal4* (FBti0002924); *l(3)31-gal4* (FBti0002096); M. Sokolowski, University of Toronto, Mississauga, ON, Canada); *OK6-gal4* (FBti0023258); B. Zhang, University of Oklahoma, Norman, OK); *UAS-nucgfp8* (FBti0012493); *GMR-gal4* (FBti0002994); *MS1096-gal4* (FBti0002374); *tub-gal4* (FBti0012687); *Df(3L)vin5* (FBab0002457). A complete description of the generation and characterization of *dube3a* mutants is in the *SI Text*.

Immunohistochemistry. Embryo immunostaining was performed as described in ref. 45. Brain immunostaining was as described at: jfly.iam.u-tokyo.ac.jp/html/manuals/pdf/E_Staining.ItoKei.pdf. Third instar larval eye disk immunostaining was as described in ref. 46. A complete list of antibodies and dilutions is in the *SI Text*. Tissues were mounted in VectaShield (Vector Laboratories). Images were acquired with a Leica SP2 AOBs or a TCS-SP confocal microscope and were manipulated by using Adobe Photoshop.

Molecular Biology. A complete description of standard methods used for *dube3a* mRNA analysis, plasmid constructions, protein blotting, and generation of Dube3a antisera is in the *SI Text*.

Behavioral Assays. Climbing (24), flight (25, 26), learning and memory (34, 35), olfaction (47), shock reactivity (48), circadian rhythm (40), and stress tests (49) were as described. Complete descriptions of each assay are in the *SI Text*.

Analysis of Eyes and Wings. Adult eyes were sectioned and photographed, and wings were mounted and photographed as described (46, 50).

ACKNOWLEDGMENTS. We thank B. Zhang, S. Waddell, X. Wang, M. Sokolowski, and J. Huibregtse for flies, help and advice, Y. Ting-Chun for help with controls, J. Huibregtse, L. Stevens, and D. Stein for plasmids, and P. Macdonald for use of his confocal microscope. This work was supported by National Institutes of Health Grants R01-HD30680 and R21-NS051307 (to J.A.F.) and R01-NS48471 (to Y.F.). F.B. received support from the Dart NeuroGenomics Alliance. A.S. is an investigator of the Howard Hughes Medical Institute.

1. Clayton-Smith J, Laan L (2003) Angelman syndrome: A review of the clinical and genetic aspects. *J Med Genet* 40:87–95.
2. Williams CA (2005) Neurological aspects of the Angelman syndrome. *Brain Dev* 27:88–94.
3. Kishino T, Lalande M, Wagstaff J (1997) *UBE3A/E6-AP* mutations cause Angelman syndrome. *Nat Genet* 15:70–73.
4. Matsuura T, et al. (1997) De novo truncating mutations in E6-AP ubiquitin-protein ligase gene (*UBE3A*) in Angelman syndrome. *Nat Genet* 15:74–77.
5. Pickart CM (2001) Mechanisms underlying ubiquitination. *Annu Rev Biochem* 70:503–533.
6. Scheffner M, Huibregtse JM, Vierstra RD, Howley PM (1993) The HPV-16 E6 and E6-AP complex functions as a ubiquitin-protein ligase in the ubiquitination of p53. *Cell* 75:495–505.
7. Vu TH, Hoffman AR (1997) Imprinting of the Angelman syndrome gene, *UBE3A*, is restricted to brain *Nat Genet* 17:12–13.

8. Rougeulle C, Glatt H, Lalande M (1997) The Angelman syndrome candidate gene, *UBE3A/E6-AP*, is imprinted in brain. *Nat Genet* 17:14–15.
9. Albrecht U, et al. (1997) Imprinted expression of the murine Angelman syndrome gene, *Ube3a*, in hippocampal and Purkinje neurons. *Nat Genet* 17:75–78.
10. Jiang Y-H, et al. (1998) Mutation of the Angelman ubiquitin ligase in mice causes increased cytoplasmic p53 and deficits of contextual learning and long-term potentiation. *Neuron* 21:799–811.
11. Cattanauch BM, et al. (1997) A candidate model for Angelman syndrome in the mouse. *Mamm Genome* 8:472–478.
12. Gabriel JM, et al. (1999) A transgene insertion creating a heritable chromosome deletion model of Prader-Willi and Angelman syndromes. *Proc Natl Acad Sci USA* 96:9258–9263.
13. Miura K, et al. (2002) Neurobehavioral and electroencephalographic abnormalities in *Ube3a* maternal-deficient mice. *Neur Disease* 9:149–159.

14. Pickart CM, Fushman D (2004) Polyubiquitin chains: Polymeric protein signals. *Curr Opin Chem Biol* 8:610–616.
15. Wang M, Pickart CM (2005) Different HECT domain ubiquitin ligases employ distinct mechanisms of polyubiquitin chain synthesis. *EMBO J* 24:4324–4333.
16. Kuhne C, Banks L (1998) E3-ubiquitin ligase/E6-AP links multicopy maintenance protein 7 to the ubiquitination pathway by a novel motif, the L2G box. *J Biol Chem* 273:34302–34309.
17. Kumar S, Talis AL, Howley PM (1999) Identification of HHR23A as a substrate for E6-associated protein-mediated ubiquitination. *J Biol Chem* 274:18785–18792.
18. Harris KF, et al. (1999) Ubiquitin-mediated degradation of active Src tyrosine kinase. *Proc Natl Acad Sci USA* 96:13738–13743.
19. Oda H, Kumar S, Howley PM (1999) Regulation of the Src family tyrosine kinase Blk through E6AP-mediated ubiquitination. *Proc Natl Acad Sci USA* 96:9557–9562.
20. Fortini ME, Skupski MP, Boguski MS, Hariharan IK (2000) A survey of human disease gene counterparts in the *Drosophila* genome. *J Cell Biol* 150:F23–F29.
21. Reiter LT, Potocki L, Chien S, Gribskov M, Bier E (2001) A systematic analysis of human disease-associated gene sequences in *Drosophila melanogaster*. *Genome Res* 11:1114–1125.
22. Reiter LT, Seagroves TN, Bowers M, Bier E (2006) Expression of the Rho-GEF Pbl/ECT2 is regulated by the UBE3A E3 ubiquitin ligase. *Hum Mol Genet* 15:2825–2835.
23. Crosby MA, et al. (2007) FlyBase: Genomes by the dozen. *Nucl Acids Res* 35:D486–D491.
24. Palladino MJ, Hadley TJ, Ganetzky B (2002) Temperature-sensitive paralytic mutants are enriched for those causing neurodegeneration in *Drosophila*. *Genetics* 161:1197–1208.
25. Talis AL, Huibregtse JM, Howley PM (1998) The role of E6AP in the regulation of p53 protein levels in human papillomavirus (HPV)-positive and HPV-negative cells. *J Biol Chem* 273:6439–6445.
26. Benzer S (1973) Genetic dissection of behavior. *Sci Am* 229:24–37.
27. Malzac P, et al. (1998) Mutation analysis of *UBE3A* in Angelman syndrome patients. *Am J Hum Genet* 62:1353–1360.
28. Fang P, et al. (1999) The spectrum of mutations in *UBE3A* causing Angelman syndrome. *Hum Mol Genet* 8:129–135.
29. Huang L, et al. (1999) Structure of an E6AP-UbcH7 complex: Insights into ubiquitination by the E2–E3 enzyme cascade. *Science* 286:1321–1326.
30. Baumer A, Balmer D, Schinzel A (1999) Screening for *UBE3A* gene mutations in a group of Angelman syndrome patients selected according to non-stringent clinical criteria. *Hum Genet* 105:598–602.
31. Lossie AC, et al. (2001) Distinct phenotypes distinguish the molecular classes of Angelman syndrome. *J Med Genet* 38:834–845.
32. Rapakko K, Kokkonen H, Leisti J (2004) *UBE3A* gene mutations in Finnish Angelman syndrome patients detected by conformation sensitive gel electrophoresis. *Am J Med Genet* 126:248–252.
33. Cooper EM, Hudson AW, Amos J, Wagstaff J, Howley PM (2004) Biochemical analysis of Angelman syndrome-associated mutations in the E3 ubiquitin ligase E6-associated protein. *J Biol Chem* 279:41208–41217.
34. Tully T, Quinn WG (1985) Classical conditioning and retention in normal and mutant *Drosophila melanogaster*. *J Comp Physiol A* 157:263–277.
35. Tully T, Preat T, Boynton SC, Del Vecchio M (1994) Genetic dissection of consolidated memory in *Drosophila*. *Cell* 79:35–47.
36. Margulies C, Tully T, Dubnau J (2005) Deconstructing memory in *Drosophila*. *Curr Biol* 15:R700–R713.
37. Yin JC, et al. (1994) Induction of a dominant negative CREB transgene specifically blocks long-term memory in *Drosophila*. *Cell* 79:49–58.
38. Yin JC, Del Vecchio M, Zhou H, Tully T (1995) CREB as a memory modulator: induced expression of a dCREB2 activator isoform enhances long-term memory in *Drosophila*. *Cell* 81:107–115.
39. DeZazzo J, et al. (2000) *nalyot*, a mutation of the *Drosophila* myb-related Adf1 transcription factor, disrupts synapse formation and olfactory memory. *Neuron* 27:145–158.
40. Rosato E, Kyriacou CP (2006) Analysis of locomotor activity rhythms in *Drosophila*. *Nat Protoc* 1:559–568.
41. Koh K, Evans JM, Hendricks JC, Sehgal A (2006) A *Drosophila* model for age-associated changes in sleep:wake cycles. *Proc Natl Acad Sci USA* 103:13843–13847.
42. Ko HW, Jiang J, Edery I (2002) Role for Slimb in the degradation of *Drosophila* Period protein phosphorylated by Doubletime. *Nature* 420:673–678.
43. Koh K, Zheng X, Sehgal A (2006) JETLAG resets the *Drosophila* circadian clock by promoting light-induced degradation of TIMELESS. *Science* 312:1809–1812.
44. Song J, Tanouye MA (2008) From bench to drug: Human seizure modeling using *Drosophila*. *Prog Neurobiol* 84:182–191.
45. Jones JR, Macdonald PM (2007) Oskar controls morphology of polar granules and nuclear bodies in *Drosophila*. *Development* 134:233–236.
46. Fischer-Vize JA, Rubin GM, Lehmann R (1992) The *fat facets* gene is required for *Drosophila* eye and embryo development. *Development* 116:985–1000.
47. Boynton S, Tully T (1992) *latheo*, a new gene involved in associative learning and memory in *Drosophila melanogaster*, identified from P element mutagenesis. *Genetics* 131:655–672.
48. Dura JM, Preat T, Tully T (1993) Identification of *linotte*, a new gene affecting learning and memory in *Drosophila melanogaster*. *J Neurogenet* 9:1–14.
49. Zhang H, et al. (2002) The *Drosophila slamdance* gene: A mutation in an aminopeptidase can cause seizure, paralysis and neuronal failure. *Genetics* 162:1283–1299.
50. Cadavid ALM, Ginzel A, Fischer JA (2000) The function of the *Drosophila* Fat facets deubiquitinating enzyme in limiting photoreceptor cell number is intimately associated with endocytosis. *Development* 127:1727–1736.